In Vivo Detection of Inflammation Using Pegylated Iron Oxide Particles Targeted at E-Selectin

A Multimodal Approach Using MR Imaging and EPR Spectroscopy

Kim A. Radermacher, MSc, Nelson Beghein, MSc,* Sebastien Boutry, PhD,† Sophie Laurent, PhD,† Luce Vander Elst, PhD,† Robert N. Muller, PhD,† Benedicte F. Jordan, PhD,* and Bernard Gallez, PhD**

Objectives: Ultrasmall particles of iron oxide (USPIO) possess superparamagnetic properties and are used as negative contrast agent in magnetic resonance imaging (MRI) because of their strong T_2 and T_2* effects. Besides this method, electron paramagnetic resonance (EPR) offers the unique capability to quantify these particles. The objective of this study was to evaluate a molecular marker for non invasive diagnosis and monitoring of inflammation. During inflammation cell adhesion molecules such as E-selectin are expressed on the endothelial cell surface. An E-selectin ligand was coupled to pegylated USPIO particles.

Materials and Methods: Inflammation was induced by intramuscular injection of Freund's Complete Adjuvant in male NMRI mice. After intravenous injection of grafted or ungrafted USPIO particles, iron concentration in inflamed muscles was quantified ex vivo by X-band EPR. Particle accumulation was also assessed in vivo by L-Band EPR, as well as by T_2-weighted MRI.

Results: We determined the mean iron oxide concentration in inflamed muscles after injection of grafted or ungrafted UPSIO particles, which was 0.8% and 0.4% of the initially injected dose, respectively. By L-band EPR, we observed that the concentration of the grafted USPIO particles in inflamed muscles was twice higher than for the ungrafted particles. Using MRI experiments, a higher signal loss was clearly observed in the inflamed muscle when grafted particles were injected in comparison with the ungrafted particles.

Conclusion: Even taking into account a non specific accumulation of iron oxides, the targeting of USPIO particles with E-selectin ligands significantly improved the sensitivity of detection of inflamed tissues.

Key Words: EPR, MRI, USPIO, molecular imaging, E-selectin

(*Invest Radiol* 2009;44: 398–404)

Molecular markers of inflammation are needed to be able to diagnose and monitor inflammation in a noninvasive manner before the occurrence of irreversible anatomic changes.[1] Physical examination is often subjective and serum markers of inflammation do not provide information about the localization of the inflamed zone.[2] Molecular markers for imaging could, therefore, be helpful in diseases where the inflammatory action of misdirected leukocytes can destroy healthy tissues, such as in atherosclerotic plaques,[3] graft rejection,[4] ischemia-reperfusion injury,[5] multiple sclerosis,[6] and rheumatoid arthritis.[7] Ultrasmall particles of iron oxide (USPIOs) have been proposed as molecular markers as these particles are phagocytosed by macrophages recruited during the inflammatory process.[3,6,8–10] This approach is, however, limited in sensitivity and specificity due to the lack of a specific target. An alternative and promising approach is to develop MR contrast agents that are selectively targeted at receptors involved in the inflammatory process.[11–13] Several cell adhesion molecules are overexpressed on leukocytes and endothelial cells during the inflammatory process.[14] Among these molecules, endothelial selectin (E-selectin) mediates the "slow rolling" of leukocytes in blood by encouraging adhesion to the vascular endothelium. This adhesion process provides the first step of granulocyte, monocyte, and T lymphocyte recruitment toward an inflamed site.[15,16] De novo E-selectin expression is stimulated by proinflammatory cytokines, like tumor necrosis factor (TNF)-α or interleukin-1β.[11,16] The up-regulation of E-selectin lasts from 4 to 30 hours after induction of inflammation and can be used as an early marker of inflammation.[15] The natural ligand of E-selectin is the tetrasaccharide, sialyl Lewis X (sLeX).[17] This carbohydrate structure is linked to certain leukocyte surface proteins by specific glycosylation enzymes.[18]

In the present study, multimodal molecular approach, with MRI and electron paramagnetic resonance (EPR) using a mimetic of the sLeX molecule coupled to a USPIO, was used to detect inflammation. This mimetic has previously been coupled with other magnetic reporters, such as gadolinium complexes, and successfully used to detect inflammation.[5,19,20] USPIOs directed against E-selectin have been proposed recently, using a coating functionalized with antibodies against E-selectin[21] or with the sLeX mimetic molecule.[22] In this study, we coupled the sLeX mimetic on USPIOs that were also coated with the hydrophilic polyethylene glycol (PEG) polymer to prolong the plasma circulation time and minimize the nonspecific accumulation of iron oxide in tissues.[23–25] The functionalized particles were characterized for their relaxometry properties and their hydrodynamic size. The ability of these functionalized particles to detect inflammation was evaluated in an in vivo model of local inflammation in muscle induced by injection of Freund's complete adjuvant (local stimulation of TNFα production). The quantitative detection of iron oxide particles in the tissues was carried out ex vivo using EPR spectroscopy. Finally, the efficacy of the targeted MR contrast agent was evaluated using in vivo EPR spectroscopy and T_2-weighted imaging.

MATERIALS AND METHODS

Synthesis of the Contrast Agent, USPIO-PEG-sLeX

USPIO-PEG750-sLeX was prepared from nanoparticles with carboxylated groups on their surface (previously described in Reference 26). The USPIOs were modified in 2 successive steps (Fig. 1): First, the USPIOs were grafted with the mimetic of the sLeX

Received December 17, 2008; and accepted for publication (after revision) March 8, 2009.

From the *Biomedical Magnetic Resonance Unit, Louvain Drug Research Institute, Brussels, Belgium; and †NMR and Molecular Imaging Laboratory, University of Mons, Mons, Belgium.

Supported by the Belgian National Fund for Scientific Research (FNRS), Televie grants (7.4597.06), the Fonds Joseph Maisin, the Saint-Luc Foundation, the "Actions de Recherches Concertées-Communauté Française de Belgique-ARC 04/09-317 and 05/10-335," and the Pôle d'attraction Interuniversitaire PAI VI (P6/38 and P6/29).

Reprints: Bernard Gallez, PhD, CMFA/REMA, Avenue Mounier 73.40, B-1200 Brussels, Belgium. E-mail: bernard.gallez@uclouvain.be.

ISSN: 0020-9996/09/4407-0398

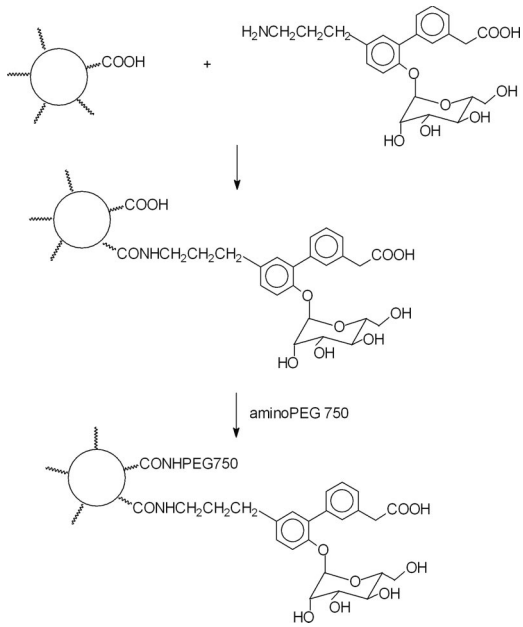

FIGURE 1. Synthetic preparation of USPIO-PEG-sLeX.

molecule;[27] second, they were coupled to aminoPEG 750 (Fluka, Bornem, Belgium).

Briefly, 10 mg of the sLeX mimetic and 6 mg of N-(3-Dimethylaminopropyl)-N′-ethylcarbodiimide hydrochloride were added to 15 mL of nanoparticles ([Fe] = 0.175 M), and the mixture was stirred overnight. The nanoparticle suspension was ultrafiltered on a 30-kD membrane. AminoPEG750 (0.503 g) and ethylcarbodiimide hydrochloride (0.327 g) were added to the nanoparticles and the reaction was stirred for 17 hours. The mixture was ultrafiltered on a 30 kD membrane to remove low-molecular weight material.

Characterization of the USPIO-PEG-sLeX

Hydrodynamic size was measured by photon correlation spectroscopy on a Brookhaven system BI-160 (New York) equipped with a He-Ne laser (λ = 633 nm, 35 mW), a goniometer, and a correlator BI-9000AT-BC. The Nuclear Magnetic Relaxation Dispersion (NMRD) profile was recorded at 37°C on a Fast Field Cycling Relaxometer (Stelar, Mede, Italy). Longitudinal relaxivities were measured over a magnetic field range from 0.24 mT to 0.24 T. The data obtained at 0.5 and 1.5 T were measured with Minispec PC-20 and Mq 60 Series systems (Bruker, Karlsruhe, Germany). The magnetization curve was recorded on a VSM-NUVO magnetometer (MOLSPIN, Newcastle Upon Tyne, UK).

Inflammatory Model

Freund's complete adjuvant was obtained from Sigma-Aldrich (Schnellendorf, Germany). FCAs are water-in-mineral oil emulsions (W/O emulsions) containing heat-killed mycobacteria (*Mycobacterium tuberculosis*, H34Ra, ATCC25177) at 1 mg/mL.

Animals and Protocol

Male NMRI mice (20–25 g) were provided by Janvier (France). For all experiments 5 to 6 mice were used per group. FCA (50 uL) was injected intramuscularly into the right rear leg (gastrocnemius muscle) of mice to stimulate E-selectin expression.[28] The left, noninflamed muscle served as control muscle. Twenty-four hours after induction of inflammation, the USPIO-PEG-sLeX or the ungrafted USPIO-PEG was injected intravenously into a tail vein at a dose of 7.7 mg Fe/kg body weight. The animal protocols were approved by the ethical committee of the Université catholique de Louvain. All experiments were conducted according to national animal care regulations.

Some commercial iron oxide particles were also studied to assess the influence of their size and coating on their kinetics. We used 3 types of preparation: ferumoxide (Guerbet; mean particle size: 80–150 nm, coating: dextran), ferucarbotran (Schering; mean particle size: 60 nm, coating: carboxydextran), and ferumoxtran-10 (Guerbet; mean particle size: 20–40 nm, coating: dextran). Each preparation was injected intravenously (7.7 mg Fe/kg) in mice. Mice were killed at different time points (5 minutes, 30 minutes, 1 hours, 2 hours, 3 hours, 5 hours, 18 hours, and 24 hours) and the iron concentrations in blood, liver, and spleen were measured by X-band EPR as described for the USPIO-PEG-sLeX.

Histology

Muscles were sampled 1, 3, and 5 hours after FCA administration, and on days 1, 3, and 7. Two mice were used for each time interval. The mice were killed by cervical dislocation, and the muscle was carefully removed. For comparison, the left gastrocnemius muscle of each mouse served as control. Muscle specimens were fixed in 10% neutral buffered formalin for 24 hours, and then embedded in paraffin. Tissues were sectioned at 5 μm and the slides were stained with hematoxylin-eosin. Analyses were performed on an optical microscope (Nikon Alphashot-2 Y52).

Ex Vivo EPR

Twenty-four hours after induction of inflammation, iron oxides were injected into the tail vein of the mice. Blood was collected by retro-orbital puncture and afterward the animals were immediately killed by cervical dislocation (time delays: 1, 3, and 6 hours). The liver, spleen, and both muscles (inflamed and control muscle) were excised. The liver and spleen samples were homogenized in NaCl 0.9% (5 times dilution). The tissue homogenates were aspirated into a Teflon capillary (5 cm long and 0.625 mm diameter), and inserted into a quartz tube that passed through the EPR cavity. As muscles cannot be homogenized easily, the muscle samples were freeze-dried, and the lyophilisate was crushed to obtain a fine powder. A Bruker EMX X-band spectrometer was used for all measurements. The instrument settings were: Fixed excitation frequency, 9.4 GHz; microwave power, 5 mW; modulation field, 100 kHz; center field, 3150 G; field width, 5000 G; modulation amplitude, 30.81 G; conversion time, 20.48 milliseconds; time constant, 20.48 milliseconds; 4096 data points and a total acquisition time of 84 seconds. Measurements were performed at room temperature. Calibration curves (using aqueous suspensions or solid material) were built with known amounts of iron oxide particles. The calibration curve for an aqueous suspension of USPIO-PEG-sLeX is shown in Figure 2.

In Vivo EPR

In vivo EPR spectra were recorded using an EPR spectrometer (Magnettech, Berlin, Germany) equipped with a low frequency microwave bridge operating at 1.2 GHz and an extended loop resonator. Twenty-four hours after FCA injection, anesthesia was induced using 3% isoflurane (in air), and then maintained using 1.8% isoflurane. USPIO-PEG-sLeX or nongrafted USPIO-PEG were injected into the tail vein. The muscles were inserted into the loop resonator, keeping the same position for all mice. In vivo EPR spectra were recorded at 1, 2, 3, and 4 hours under the following conditions: Fixed excitation frequency, 1.2 GHz; microwave power, 24 mW; modulation field, 100 kHz; center field, 53 mT; field width, 20 mT; modulation amplitude, 0.42 mT; 1024 data points and a total acquisition time of 60 seconds.

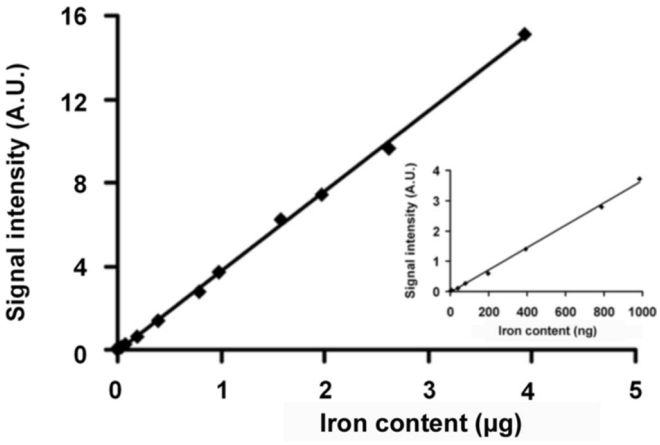

FIGURE 2. Quantitative analysis of iron oxide by EPR spectrometry. Calibration curve of the signal intensity as a function of iron content.

In Vivo MRI

Twenty-four hours after FCA injection, the animals were anesthetized with isoflurane (3% induction, 1.8% maintenance). MR images were obtained on a Bruker BIOSPEC system equipped with a horizontal 4.7 T magnet. The images were acquired using a T_2-weighted RARE sequence. The parameters were repetition time, TR = 3.2 seconds; echo time, TE, 66.9 milliseconds; bandwidth, 50 kHz; FOV, 5 cm; matrix size, 128 × 128; 2-mm slice thickness; acquisition time, 6 minutes 49 seconds. After a precontrast sequence, USPIO-PEG-sLeX or nongrafted USPIO-PEG were injected into the tail vein of the mice. Postcontrast images of the muscles were acquired at different time delays (every 30 minutes until 3 hours) after injection of the iron oxides. As a control, we placed a phantom tube containing $CuSO_4$ (100 mg/L) alongside the animals and measured the phantom signal before and after the contrast media injection. For the analysis, Paravision software was used to measure the signal intensities (SI) in the different regions of interest chosen in the control muscle, the inflamed muscle, and the phantom. Muscle SI was normalized to the SI of the phantom, yielding a relative intensity (RI) for each muscle. Negative contrast enhancement values were calculated for each time point using the following equation:

$$\% \text{ enhancement values} = ([\text{RI post} - \text{RI pre}])/\text{RI pre}) \times 100.$$

For MRI data analysis the T_2 relaxation time has been calculated from the multispin-echo datasets using in-house software based on the interactive data language (Research Systems, Boulder, CO). Regions of interest were drawn within the inflamed tissue and the mean T_2 value was calculated before and after contrast-enhancement of the inflamed muscles to evaluate the T_2 shortening produced by the grafted or ungrafted USPIO particles.

Statistical Analysis

All results are given as mean values ± SEM from 5 to 6 animals per group. Comparisons between groups were made with Student 2-tailed *t* test and a $P < 0.05$ was considered as significant. The following symbols are used in the figures: $*P < 0.05$, $**P < 0.01$, $***P < 0.001$.

RESULTS

Characterization of the USPIO-PEG-sLeX

The hydrodynamic size of the synthesized USPIO-PEG-sLeX was 23 nm (polydispersity index = 0.128). The R_1-NMRD profile of USPIO-PEG-sLeX is shown in Figure 3 (left). The relaxivity values at 37°C were: $r_1 = 36.8\ mM^{-1}s^{-1}$ and $r_2 = 87.2\ mM^{-1}s^{-1}$ (at 20 MHz), and $r_1 = 15.4\ mM^{-1}s^{-1}$ and $r_2 = 87.8\ mM^{-1}s^{-1}$ (at 60 MHz). The relaxivity is defined as relaxation rate of water protons in 1 mmol/L solution of contrast agents and its value is expressed in mmol/L in iron. Interpretation of the relaxation profiles (ie, evolution of the relaxivity as a function of the magnetic field) with appropriate theoretical models[29,30] provides information about the main properties of the superparamagnetic crystals, such as their specific magnetization (51.7 Am^2/kg) and their size (d = 11.6 nm). The corresponding values obtained by magnetometry (Fig. 3, right) were Ms = 68.3 Am^2/kg for the magnetization and d = 9.8 nm for the crystal diameter. As previously observed, the mean diameter obtained by magnetometry was less than that obtained by relaxometry. This difference can be explained by a distribution of crystal sizes, which influences the mean size obtained by the various methods.[31] This size dispersion is also responsible for the lower specific magnetization obtained by relaxometry compared with that obtained by magnetometry.

Inflammatory Model

Histologic analysis confirmed the presence of a large area of inflammation in the muscle injected with FCA. Inflammatory cells were recruited near the site of injection which was identified by remaining droplets of mineral oil. Inflammatory cell recruitment was already visible 1 hour after administration of FCA, increased progressively up to 1 day after injection, and then remained unchanged on days 3 and 7. A typical histologic image (obtained 1 day after injection of FCA) is shown in Figure 4. As it was established that E-selectin is highly up-regulated in this inflammatory model,[28] and as the up-regulation lasts from 4 to 30 hours after induction of the

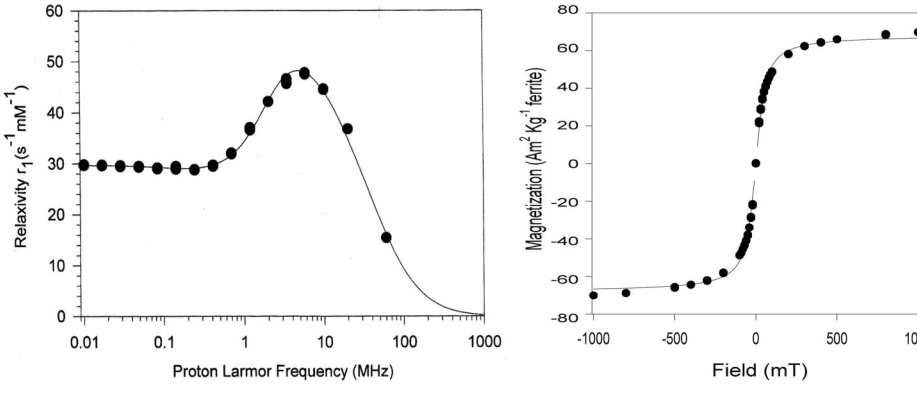

FIGURE 3. Magnetic characterization of USPIO-PEG-sLeX. Left: NMRD profile. Right: magnetometry curve.

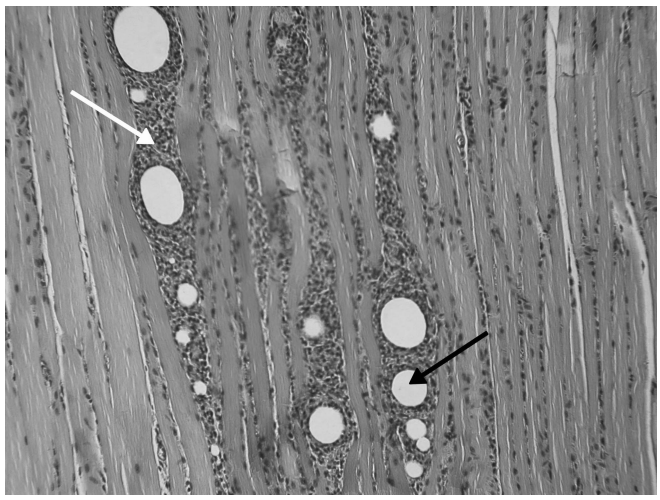

FIGURE 4. Histologic image of an inflamed mouse muscle 24 hours after administration of 50 uL of Freund's Complete Adjuvant. The white arrow indicates the inflammatory cells recruited on the inflamed site and the black arrow shows small lipid bubbles of remaining mineral oil.

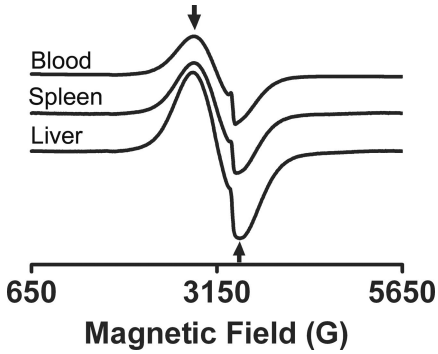

FIGURE 5. Typical EPR X-band spectra of the different tissues recorded ex vivo at 3 hours after IV injection of USPIO-PEG-sLeX.

inflammation, we further used 24 hours after injection of FCA to evaluate the distribution of the USPIOs.

Ex Vivo EPR

USPIOs exhibit an EPR spectrum, which directly reflects the number of iron oxide particles in a sample (Fig. 2). EPR spectroscopy has already been proposed as a method of quantifying the accumulation of iron oxide inside tissues.[32] Calibration curves were built from saline and liver homogenates containing known concentrations of iron oxide particles. The calibration curves did not change when the particles were dispersed in saline or in liver homogenates (data not shown). The EPR spectra were characterized by an average *g* value of 2.13. Typical EPR spectra recorded in different tissues (blood, spleen, and liver) are shown in Figure 5. The evolution of the concentration of USPIO-PEG-sLeX in different tissues is shown in Figure 6. In blood (Fig. 6, left), we observed a decrease in circulating USPIO-PEG-sLeX over time. The iron oxide remaining in the circulation 1 hour after IV injection, expressed as a percentage of the initial blood concentration just after injection, was 17.7% ± 0.7% for USPIO-PEG-sLeX and 17.5% ± 0.8% for USPIO-PEG (mean ± SEM, n = 5). Under the same conditions, the remaining circulating

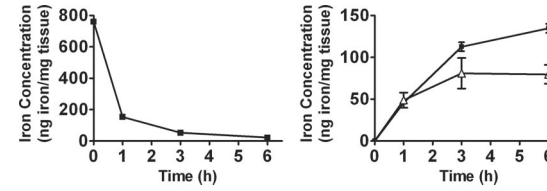

FIGURE 6. Time course of USPIO-PEG-sLeX concentration in different tissues as measured by ex vivo X-band EPR spectroscopy. Left: measurements in blood (■). Right: measurements in the liver (▲) and in the spleen (Δ). The results are expressed as mean ± SEM, n = 5.

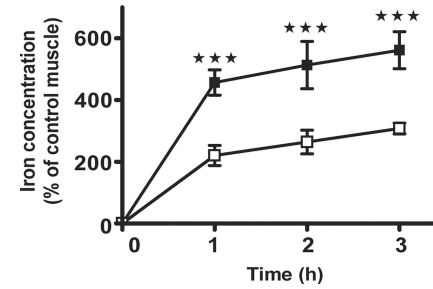

FIGURE 7. Time course of USPIO-PEG (□) and USPIO-PEG-sLeX (■) concentration in inflamed muscle as measured by X-band EPR ex vivo. The results are expressed as % of the concentration found in control muscle (mean ± SEM, n = 5).

iron oxides were 4.7% ± 0.4%, 2.7% ± 0.2%, and 0.9% ± 0.1% of the initial blood concentration for ferumoxtran-10, ferucarbotran, and ferumoxide, respectively. The concentration of USPIO-PEG-sLeX was less than 3% after 6 hours, and it was completely cleared from the blood 24 hours after administration (data not shown). In the spleen, the concentration of USPIO-PEG-sLeX reached a plateau by 3 hours after injection and then remained stable for the rest of the observation period (6 hours). In the liver, the concentration of USPIO-PEG-sLeX increased over time, but the rate of accumulation appeared to slow slightly 3 hours after administration. After this preliminary USPIO-PEG-sLeX biodistribution study, we evaluated the inflamed muscles. The results are expressed as a percentage of the iron oxide concentration detected in the noninflamed control muscle (Fig. 7). The accumulation of iron oxide particles in the inflamed muscle was significantly higher after administration of USPIO-PEG-sLeX compared with ungrafted USPIO-PEG. Three hours after injection of the contrast media, the mean muscular iron content was 561% ± 60% (mean ± SEM, n = 5) for mice injected with USPIO-PEG-sLeX, and 308% ± 18% for mice injected with ungrafted USPIO-PEG. In other words, the iron content was about 6 times higher in the inflamed muscle than in the control muscle, using USPIO-PEG-sLeX, and when using USPIO-PEG control particles, iron concentration is still 3 times higher in inflamed muscles than in control muscles. The amount of iron accumulated in the inflamed muscle was about 0.8% of the injected dose when using USPIO-PEG-sLeX compared with 0.4% obtained with USPIO-PEG particles.

In Vivo EPR

Using EPR spectrometers operating at low frequency, it is possible to record EPR spectra directly in vivo. We looked at the feasibility of detecting USPIO directly in vivo using these systems. Interestingly, the EPR signal was easily visible in inflamed muscles,

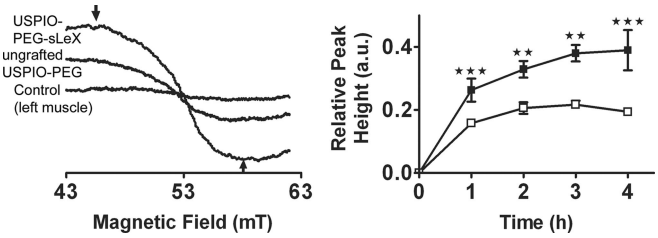

FIGURE 8. In vivo EPR study after administration of the USPIOs. Left: typical EPR L-band spectra recorded at 3 hours after USPIO injection. Right: Mice with inflamed muscle were injected with either USPIO-PEG-sLeX (■) or with USPIO-PEG as control particles (□) and time course of iron concentration in inflamed muscles was measured by L-band EPR. Results are expressed as mean ± SEM, n = 6 mice/group.

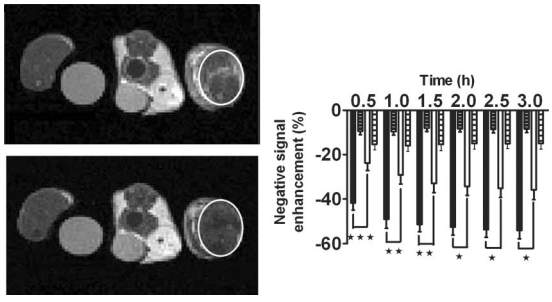

FIGURE 9. Effect of the USPIOs on the MR contrast in inflamed muscle. Left: typical T_2-weighted images before (top) and 3 hours after (bottom) the administration of USPIO-PEG-sLeX. The control muscle is located on the left, the inflamed muscle on the right. The white circles indicate the regions of interest in the inflamed muscles with an obvious signal decrease after administration of USPIO-PEG-sLeX. Right: bar graph showing the time course of the negative contrast enhancement produced by USPIO-PEG-sLeX (black) and ungrafted USPIO-PEG (white) in T_2-weighted images. The effect on the control muscle is indicated by the striped bar graph. Results are mean ± SEM, n = 5 mice/group.

compared with control muscles (Fig. 8, left). The SI was measured as a function of time (Fig. 8, right). Between 3 and 4 hours after the injection, the SI recorded in the inflamed muscle was twice as high with USPIO-PEG-sLeX as with ungrafted USPIO-PEG.

In Vivo MRI

Iron oxide particles are characterized by a large magnetic moment and a large size that leads to a shortening of the transverse relaxation time (T_2) and to considerable signal loss in T_2-weighted MRI sequences. MR images were obtained before and at different times following the intravenous administration of iron oxide particles (Fig. 9, left). The SI decreased rapidly in the inflamed muscle after administration of USPIO-PEG-sLeX. The signal loss was −49% ± 4% 60 minutes after the administration of the contrast agent, and remained stable until the end of the 3 hours imaging period (−54% ± 4%). The decrease in SI was less pronounced when using the ungrafted USPIO-PEG (−36% ± 4%). There was also a small, but significant, decrease in SI in the control muscle (around 10%) after injection of both contrast media.

Calculated T_2 values were obtained from mice before and 3 hours after administration of either USPIO-PEG-sLeX or USPIO-PEG. The shortening of the transversal relaxation time T_2 in inflamed mice muscle is about 41.8 ± 5.2 milliseconds when targeted particles were injected and only 21.1 ± 5.1 milliseconds for the untargeted ones (Fig. 10). Compared with the T_2 value measured on precontrast images the particles produce a T_2 shortening of 62.9% and 37.3%, respectively, which kind of reconfirms the percentages obtained for the negative signal enhancement.

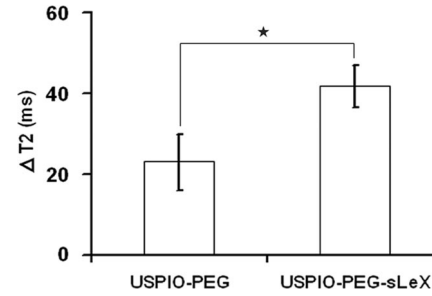

FIGURE 10. The graph shows mean ΔT_2 measurements of either targeted or untargeted USPIO particles, with $\Delta T_2 = T_2$ precontrast—T_2 3 hours postcontrast.

DISCUSSION

The major insights of the present study are (*a*) EPR and MRI can be used complementarily to assess the amount and localization of targeted iron oxide particles; (*b*) USPIO-PEG-sLeX accumulate preferentially in inflamed areas, and may be used as inflammation-selective MR contrast agents.

Multimodality approach involves the incorporation of at least 2 measuring modalities using labeled "reporter" agents. Useful complementary information coming from a multimodal approach may be related to localization (macroscopic imaging or histology), absolute quantification, metabolism, or gene activation. NMR spectroscopy and imaging are able to provide important anatomic, functional, and metabolic imaging, with very high spatial resolution for several nuclei. To measure real concentrations of iron oxide in tissues, other authors have used the incorporation of radioactive ^{59}Fe in the USPIO core[33] or inductively coupled plasma-atomic emission spectrometry.[34] Here, we used EPR, a magnetic resonance method that detects the presence of species carrying unpaired electrons with high sensitivity. EPR spectrometry is interesting because it is more sensitive than NMR (due to the difference in gyromagnetic ratio) and because the EPR signal intensity quantitatively reflects the amount of iron oxide particles, without any confounding effect. Calibration curves were built with standard amounts of iron oxide contrast agent to check the linearity of the response (Fig. 2). EPR is generally used in vitro or ex vivo on freeze-dried samples or thin tissue homogenates to avoid the dielectric loss observed in large aqueous samples. Early work carried out on magnetite particles in the nineties indicated that X-Band EPR was useful to monitor the clearance of iron oxide particles from the blood[32] and their accumulation in the liver and in the spleen by ex vivo sampling.[35] To correlate the dynamics observed in MRI with EPR, we also used a low frequency EPR spectrometer (1GHz) that allows a wave penetration of 1 cm inside tissue, which was typically the size of the muscles analyzed in the present study. To our knowledge, only one in vivo study has reported the detection of superparamagnetic iron oxide particles in the liver using an L-band spectrometer.[36] So far, EPR has never been used in the evaluation of targeted iron oxide particles developed for molecular imaging.

To conduct a fair comparison between USPIO-PEG-sLeX and USPIO-PEG, we first checked the EPR and NMR characteristics of both iron oxide contrast agents. The r_2 relaxivities obtained for

USPIO-PEG-sLeX are comparable to values obtained previously with ungrafted USPIO-PEG or USPIO grafted with sLeX without pegylation of the particles.[22] This finding confirms that the branching did not induce a major change in the relaxometric properties of these compounds. We also observed that the EPR signal intensity and shape were not dependent on the coating of the surface of the particle, nor on the tissue in which the USPIO was dispersed. This observation allowed us to quantify and compare directly the content of the contrast agent in different tissues.

The change in blood clearance as a result of the branching of PEG polymers at the surface of the particles is obvious when the amount of iron oxide particles remaining in the circulating blood is compared for different preparations. Comparison with ferumoxtran-10 is the most relevant as this compound has a size (20–40 nm) comparable to that of USPIO-PEG-sLeX (23 nm). One hour after administration, the blood concentration of USPIO-PEG-sLeX (and of the ungrafted USPIO-PEG) was about 4 times higher than the blood concentration of ferumoxtran-10. The PEG chains, which are known to reduce plasma protein binding (opsonization), do indeed delay clearance by macrophages. It should be noted that the pegylation did not preclude the final accumulation of USPIOs in the reticulo-endothelial system as we observed a large uptake by the liver and the spleen (Fig. 6). Nevertheless, the increased half-life in the blood is beneficial to the possible molecular recognition of targeted sites.

To estimate the ability of USPIO-PEG-sLeX to specifically detect local inflammation, we used ex vivo EPR, in vivo EPR and MRI. Ex vivo EPR allowed the absolute quantification of iron oxide particles in tissues by comparison with standard calibration curves (Fig. 2). Interestingly, we obtained in vivo EPR signals from USPIOs with a high signal-to-noise ratio using rapid scans (1 minute) in a noninvasive manner. It should be emphasized that the absolute quantification by EPR is theoretically more difficult to obtain in vivo than ex vivo, as the signal strongly depends on the geometry of detection. However, we obtained a reasonable quantification by carefully placing the leg muscle in exactly the same position from one study to another. The results obtained by both techniques (Figs. 7, 8) are remarkably concordant. Finally, MRI studies were carried out to evaluate the ability of this new contrast agent to improve the contrast in inflamed tissues. The 3 methods led to the same conclusions: (1) the ungrafted USPIO-PEG was more concentrated in inflamed muscles than in control muscles; (2) there was a higher accumulation (by a factor 2) of USPIO-PEG-sLeX compared with ungrafted USPIO-PEG in inflamed areas. The large concentration of ungrafted USPIO-PEG in inflamed muscles as compared with control muscles can be explained by the fact that inflamed muscle will recruit a large number of macrophages. These macrophages will take up USPIOs in a nonspecific manner. Furthermore, inflammation causes vasodilation and increased vascular permeability. The resulting improvement in blood flux and transendothelial passage enables a greater accumulation of iron oxide particles in the inflamed tissue. Even taking into account the nonspecific accumulation of USPIOs in local macrophages, our results clearly indicate that the use of USPIO-PEG-sLeX improved the ability to detect inflammation by a factor of 2 compared with ungrafted USPIO-PEG.

In conclusion, USPIO-PEG-sLeX shows promise as an in vivo tool for the noninvasive analysis of the expression of E-selectin in different disorders. The long intravascular persistence time, selective accumulation in inflamed tissues, and the high and prolonged contrast provided in MRI studies support further studies using this new type of contrast agent.

REFERENCES

1. Rennen HJ, Boerman OC, Oyen WJ, et al. Imaging infection/inflammation in the new millenium. *Eur J Nucl Med*. 2001;28:241–252.
2. Dardzinski BJ, Schmithorst VJ, Holland SK, et al. MR imaging of murine arthritis using ultrasmall superparamagnetic iron oxide particles. *J Magn Reson Imag*. 2001;19:1209–1216.
3. Kooi ME, Cappendijk VC, Cleutjens KB, et al. Accumulation of ultrasmall superparamagnetic particles of iron oxide in human atherosclerotic plaques can be detected by in vivo magnetic resonance imaging. *Circulation*. 2003;107:2453–2458.
4. Beckmann N, Cannet C, Fringeli-Tanner M, et al. Macrophage labeling by SPIO as an early marker of allograft chronic rejection in a rat model of kidney transplantation. *Magn Reson Med*. 2003;49:459–467.
5. Barber PA, Foniok T, Kirk D, et al. MR Molecular imaging of early endothelial activation in focal ischemia. *Ann Neurol*. 2004;56:116–120.
6. Dousset V, Brochet B, Deloire MS, et al. MR imaging of relapsing multiple sclerosis patients using ultra-small-particle iron oxide and compared with gadolinium. *Am J Neuroradiol*. 2006;27:1000–1005.
7. Tanaka Y. The role of chemokines and adhesion molecules in the pathogenesis of rheumatoid arthritis. *Drugs Today (Barc)*. 2001;37:477–484.
8. Dousset V, Delalande C, Ballarino L, et al. In vivo macrophage activity imaging in the central nervous system detected by magnetic resonance. *Magn Reson Med.* 1999;41:329–333.
9. Ruehm SG, Corot C, Vogt P, et al. Magnetic resonance imaging of atherosclerotic plaque with ultrasmall superparamagnetic particles of iron oxide in hyperlipidemic rabbits. *Circulation*. 2001;103:415–422.
10. Frericks BB, Wacker F, Loddenkemper C, et al. Magnetic resonance imaging of experimental inflammatory bowel disease: quantitative and qualitative analyses with histopathologic correlation in a rat model using the ultrasmall iron oxide SHU 555 C. *Invest Radiol*. 2009;44:23–30.
11. Kang HW, Josephson L, Petrovsky A, et al. Magnetic resonance imaging of inducible E-selectin expression in human endothelial cell culture. *Bioconjug Chem*. 2002;13:122–127.
12. Alsaid H, De Souza G, Bourdillon MC, et al. Biomimetic MRI contrast agent for imaging of inflammation in atherosclerotic plaque of ApoE−/− mice: a pilot study. *Invest Radiol.* In press.
13. Zheng J, Ochoa E, Misselwitz B, et al. Targeted contrast agent helps to monitor advanced plaque during progression: a magnetic resonance imaging study in rabbits. *Invest Radiol*. 2008;43:49–55.
14. Albelda SM, Buck CA. Integrins and other cell adhesion molecules. *FASEB J*. 1990;4:2868–2880.
15. Leeuwenberg JF, Smeets EF, Neefjes JJ, et al. E-selectin and intercellular adhesion molecule-1 are released by activated human endothelial cells in vitro. *Immunology*. 1992;77:543–549.
16. Wyble CW, Hynes KL, Kuchibhotla J, et al. TNF-α and IL-1 upregulate membrane-bound and soluble E-selectin through a common pathway. *J Surg Res*. 1997;73:107–112.
17. Foxall C, Watson SR, Dowbenko D, et al. The three members of the selectin receptor family recognize a common carbohydrate epitope, the sialyl Lewis(x) oligosaccharide. *J Cell Biol*. 1992;117:895–902.
18. Vestweber D, Blanks JE. Mechanisms that regulate the function of the selectins and their ligands. *Physiol Rev*. 1991;79:181–213.
19. Sibson NR, Blamire AM, Bernades-Silva M, et al. MRI detection of early endothelial activation in brain inflammation. *Magn Reson Med.* 2004;51:248–252.
20. Boutry S, Burtea C, Laurent S, et al. Magnetic resonance imaging of inflammation with a specific selectin-targeted contrast agent. *Magn Reson Med*. 2005;53:800–807.
21. Reynolds PR, Larkman DJ, Haskard DO, et al. Detection of vascular expression of E-selectin in vivo with MR Imaging. *Radiology*. 2006;241:469–476.
22. Boutry S, Laurent S, Elst LV, et al. Specific E-selectin targeting with a superparamagnetic MRI contrast agent. *Contrast Media Mol Imaging.* 2006;1:15–22.
23. Oussoren C, Storm G. Lymphatic uptake and biodistribution of liposomes after subcutaneous injection: III. Influence of surface modification with poly(ethyleneglycol). *Pharm Res*. 1997;14:1479–1484.
24. Veronese FM, Mero A. The impact of PEGylation on biological samples. *BioDrugs*. 2008;22:315–329.
25. Jain A, Jain SK. PEGylation: an approach for drug delivery. A review. *Crit Rev Ther Drug Carrier Syst*. 2008;25:403–447.
26. Port M, Corot C, Raynal I, et al. Novel compositions magnetic particles covered with gem-bisphosphonate derivatives. US Patent 0253181 A1. 2004.
27. Fu Y, Laurent S, Muller RN. Synthesis of a Sialyl Lewis X mimetic conjugated with DTPA, potential ligand of new contrast agents for medical imaging. *Eur J Org Chem.* 2002;3966–3873.

28. Machelska H, Brack A, Mousa SA, et al. Selectins and integrins but not platelet-endothelial cell adhesion molecule-1 regulate opioid inhibition of inflammatory pain. *Br J Pharmacol*. 2004;142:772–780.
29. Roch A, Muller RN, Gillis P. Theory of proton relaxation induced by superparamagnetic particles. *J Chem Phys*. 1999;110:5403–5411.
30. Roch A, Gillis P, Ouakssim A, et al. Proton relaxation in superparamagnetic aqueous colloids: a new tool for the investigation of ferrite crystal anisotropy. *J Magn Magn Mater*. 1999;201:77–79.
31. Ouakssim A, Fastrez S, Roch A, et al. Control of the synthesis of magnetic fluids by relaxometry and magnetometry. *J Magn Magn Mater*. 2004;272–276:E1711–E1713.
32. Iannone A, Federico M, Tomasi A, et al. Detection and quantitation in rat tissues of the superparamagnetic magnetite resonance contrast agent dextran magnetite as demonstrated by electron spin resonance spectroscopy. *Invest Radiol*. 1992;27:450–455.
33. Weissleder R, Elizondo G, Wittenberg J, et al. Ultrasmall superparamagnetic iron oxide: characterization of a new class of contrast agents for MR imaging. *Radiology*. 1990;175:489–493.
34. Raynal I, Prigent P, Peyramaure S, et al. Macrophage endocytosis of superparamagnetic iron oxide nanoparticles: mechanisms and comparison of ferumoxides and ferumoxtran-10. *Invest Radiol*. 2004;39:56–63.
35. Iannone A, Magin RL, Walczak T, et al. Blood clearance of dextran magnetite particles determined by a noninvasive in vivo ESR method. *Magn Reson Med*. 1991;22:435–442.
36. Fujii H, Yoshikawa K, Berliner LJ. In vivo fate of superparamagnetic iron oxides during sepsis. *J Magn Reson Imaging*. 2002;20:271–276.